Mitonuclear interactions impact aerobic metabolism in hybrids and may explain mitonuclear discordance in young, naturally hybridizing bird lineages

Authors: Callum S. McDiarmid[1], Daniel M. Hooper[2*], Antoine Stier[3,4], Simon C. Griffith[1]

[1] School of Natural Sciences, Macquarie University, Sydney, NSW, Australia; [2] Institute for Comparative Genomics, American Museum of Natural History, New York, NY, USA; [3] Department of Biology, University of Turku, Turku, Finland; [4] Institut Pluridisciplinaire Hubert Curien, UMR7178, Université de Strasbourg, CNRS, Strasbourg, France

*correspondence: dhooper@amnh.org

Keywords: speciation, mitochondrial, aerobic respiration, hybridization, cyto-nuclear discordance

Abstract

Understanding genetic incompatibilities and genetic introgression between incipient species are major goals in evolutionary biology. Mitochondrial genes evolve rapidly and exist in dense gene networks with coevolved nuclear genes, suggesting that mitochondrial respiration may be particularly susceptible to disruption in hybrid organisms. Mitonuclear interactions have been demonstrated to contribute to hybrid disfunction between deeply divergent taxa crossed in the laboratory, but there are few empirical examples of mitonuclear interactions between younger lineages that naturally hybridise. Here we use experimental crosses and high resolution respirometry to provide the first evidence in a bird that inter-lineage mitonuclear interactions impact mitochondrial aerobic metabolism. Specifically, respiration capacity of the two paternal backcrosses (with mismatched mito-nuclear combinations) differ from one another, although they do not differ to the parental groups or maternal backcrosses as we would expect of mitonuclear disruptions. In the wild hybrid zone between these subspecies the mitochondrial cline centre is shifted west of the nuclear cline centre, which is consistent with the direction of our experimental results. Our results therefore demonstrate asymmetric mitonuclear interactions that impact the capacity of cellular mitochondrial respiration and may help to explain the geographic discordance between mitochondrial and nuclear genomes observed in the wild.

Introduction

Understanding the factors that obstruct gene flow or propel genetic introgression between biological lineages is a central goal of speciation research[1]. One factor that may be particularly susceptible to disruption in hybrids is the interaction between the mitochondrial and nuclear genomes, which underpin mitochondrial aerobic metabolism[2–4]. Functional mitochondria rely on dense gene networks encompassing genes in both the mitochondrial (N= ~37 genes) and nuclear (N = ~1,500 genes) genomes (Figure 1A)[5–7], and these genes (particularly mitochondrial genes) can undergo rapid synonymous change between lineages [8–12]. Following hybridization, novel combinations of mtDNA and nuDNA may disrupt mitochondrial function and thus act as a reproductive isolating barrier.

Inter-lineage mitonuclear interactions – i.e., interactions between the mitochondria of one lineage and the nuclear genome of another lineage that occur within the cells of hybrids - have been demonstrated to contribute to hybrid disfunction between deeply divergent taxa crossed in the laboratory [13–17]. There are, however, fewer empirical examples of inter-lineage mitonuclear interactions between younger taxa that naturally hybridise [18–20]. In birds, there is suggestive evidence from hybrid zones that mitonuclear incompatibilities may contribute to reproductive isolation [21–23]. Direct evidence linking hybrid disfunction with mitonuclear incompatibilities is lacking, however, in large part because most birds cannot be readily kept and bred in captivity. This precludes controlled experiments to effectively disassociate the mitochondrial and nuclear genomes. Naturally produced hybrids that have low physiological function may be compromised for various other reasons, such as their parents mating with a heterospecific because they were poor quality individuals [24]. In contrast to genetic incompatibilities of uniform effect on hybrid fitness, interactions of asymmetrical effect [i.e., differential fitness between hybrids based on direction of cross] can result in certain genes introgressing beyond the hybrid zone and geographic discordance between different regions of the genome. In naturally hybridizing systems, geographic discordance between mtDNA and nuDNA is observed at an appreciable frequency but the underlying mechanisms are rarely understood[25]. Discordance is often attributed to demographic disparities or sex-biased asymmetries based mostly on verbal arguments[26], while the functional consequences of mitonuclear interactions such as those described here are rarely considered [25,27,28].

Optimal function of mitochondrial respiration in birds is dependent on 37 genes in the mtDNA, including 13 protein coding genes that encode key components of the well characterised complexes

I, III, IV and V in the electron transport system (ETS) on the inner mitochondrial membrane. In addition, avian mtDNA encodes two ribosomal RNAs (rRNAs), 22 transfer RNAs (tRNAs) and a control region (OH). In humans, for example, disfunction of these mitochondrial genes can impact fitness and manifest as mitochondrial diseases and disorders such as neurodegeneration[29,30]. Changes in the amino acid composition of ETS subunits, or genetic substitutions in the tRNA or rRNA machinery that impact the transcription or translation of ETS subunits, can both potentially destabilise the transfer of high-energy electrons causing them to leak from the ETS. Leaking electrons can contribute to the formation of reactive oxygen species (ROS) that can damage cellular macromolecules[30].

The subspecies of the long-tailed finch *Poephila acuticauda acuticauda* and *P. a. hecki* inhabit tropical savannahs across northern Australia and naturally hybridise where their distributions meet on the edge of the Kimberley Plateau in Western Australia[31]. Previous work has estimated they last shared a common ancestor approximately 0.5 million years ago (0.31 – 0.68 Mya, 95% HPD) based on divergence in three mtDNA genes[32]. Mitonuclear discordance has been observed in the wild hybrid zone between these two subspecies, with the centre of the mitochondrial cline being 55 km west of the nuclear cline centre[32], but within the boundaries of the nuclear hybrid zone (Figure 1B & C, [32]). This discordance suggests the eastern mitochondrial lineage (mitotype) has introgressed westward across the hybrid zone. One possible explanation for this apparent introgression is that hybridisation causes novel mitonuclear interactions that asymmetrically reduce the fitness of individuals with a western mitotype and eastern nuclear genome, by adversely impacting aerobic metabolism and therefore ATP synthesis, or through elevated generation of reactive oxygen species (ROS) that results in oxidative stress. The long-tailed finch can be readily kept and bred in captivity, making it an experimentally tractable model system in which to examine the consequences of this potential mitonuclear mismatch.

Here, we test whether inter-lineage mitonuclear interactions impact aerobic metabolism using subspecies of the long-tailed finch. We utilized a cross design that should expose any inter-lineage mitonuclear interactions that exist between the subspecies in the resulting hybrid embryos. We then assessed mitochondrial aerobic respiration capacity using high-resolution respirometry[33].

Methods

Study species

Long-tailed finches of each subspecies (*Poephila acuticauda acuticauda* and *P. a. hecki*) used in this study came from captive populations maintained at Macquarie University in Sydney, Australia. Wild caught *P. a. acuticauda* individuals were originally sourced from Mount House (17°02'S, 125°35'E) and Nelson's Hole (15°49'S, 127°30'E) in Western Australia, and wild-caught *P. a. hecki* were sourced from October Creek (16°37'S, 134°51'E) in the Northern Territory[34,35]. As individuals from these populations show no evidence of genomic admixture between subspecies[31,32] we hereafter refer to them as 'parental'.

mtDNA comparison between subspecies

Changes in the mitochondrial genome are required but not sufficient for inter-lineage mitonuclear incompatibility. Even a single substitution in the mtDNA can lead to reproductive isolation (e.g., [48]). To identify substitutions with the potential to contribute to incompatibilities, we sequenced whole mitochondrial genomes from each long-tailed finch subspecies and counted the number of fixed differences and associated amino acid changes within 13 protein coding genes between them. We assembled mitochondrial genomes using whole genome sequence (WGS) data from both long-tailed finch subspecies (*P. a. acuticauda,* N = 14; *P. a. hecki* N = 11) and their sister species the black-throated finch *P. cincta atropygialis* (N = 11). We used bcftools (version 1.9)[49] consensus after calling and incorporating variants relative to the zebra finch reference genome (GCA_003957565.4) in each sample. Ambiguous positions were output with associated IUPAC codes[43]. We exclusively used WGS data derived from DNA extracted from muscle (rather than blood) to ensure that they were enriched for reads from mitochondrial DNA and not reads from the nuclear encoded mtDNA (NUMT) copy. The mitochondrial genome of the zebra finch reference was used as an additional outgroup to help assign substitutions to their lineage of origin. We used the MITOS2 WebServer[50] to extract specific sequences for each mtDNA encoded gene, including all 13 protein coding genes, 22 tRNA and 2 rRNA and the control region. Each gene was aligned using MAFFT (version 7) web-aligner[51] and we manually examined each alignment with Geneious prime (version 2023.1.2) to count and characterize the distribution of fixed differences between each of the three members of *Poephila* (Table S1). For each protein-coding gene, we used the number of fixed differences between subspecies to quantify their absolute divergence (D_{XY}).

We next evaluated the extent of non-synonymous change between long-tailed finch subspecies for each protein-coding gene. We generated lineage-specific consensus sequences for each gene and used the vertebrate mitochondrial genetic code to translate these to amino acid sequence. We again used data from the black-throated finch and zebra finch as outgroups to assign

131 amino acid changes to the long-tailed finch subspecies of origin. We classified each amino acid
132 substitution by any associated change in biochemical properties. Finally, we calculated the ratio of the
133 rate of non-synonymous to the rate of synonymous nucleotide substitutions (dN/dS) between long-
134 tailed finch subspecies for each protein-coding gene using the model M0 implemented in the program
135 Easy-CodeML (v1.41)[52].
136
137 **Breeding**
138 Embryos were produced by rotating pairs of long-tailed finches through 20 outdoor aviaries (4.1 m
139 long x 1.85 m wide x 2.24 m high), with one pair per aviary containing nest boxes and nesting material.
140 Mealworms, greens, dry seed, and water were provided *ad libitum*. We required females to have been
141 exclusively with the partner for 14 days minimum before any experimental eggs were collected, to
142 avoid embryos being sired by stored sperm from a different male. Nest boxes were checked every day
143 and eggs were collected the day they were laid, given a unique number using a permanent marker,
144 and stored in a 'soft box' at cool room temperature (22 °C) for up to seven days before being placed
145 into an incubator (Brinsea Ovation 56 EX, Brinsea Products, Winscombe, U.K.). Eggs were incubated
146 at 37.5°C and 65% humidity for 12 days. On the 12th day (i.e., the day before expected hatch) eggs
147 were removed and measurements made. Working with embryos meant we eliminated the
148 opportunity for the effects of extended parental care by parents of different genetic backgrounds.
149
150 **Crossing Design**
151 We produced backcrossed offspring by first breeding F_1 hybrid females with an unadmixed parental
152 male of each subspecies, sequentially and in random order. Resulting offspring were defined as
153 maternal backcrosses if their father's lineage *did* match their mother's mitotype and were defined as
154 paternal backcrosses if father's lineage *did not* match their mother's mitotype (Figure 2). Parental
155 pairs of each subspecies were set up to breed at the same time and used as controls.
156
157 Paternal backcrossing exposes incompatibilities by producing offspring who inherit most of
158 their nuclear genome from a different lineage to that of their mitochondrial genome. This is
159 particularly pronounced in the case of the long-tailed finch, as >98.5% of fixed nuclear differences
160 between subspecies are on the Z-chromosome[36]. In our cross design, paternal backcross offspring
161 inherit Z chromosomes that have had no opportunity for recombination between subspecies. If male,
162 they receive one Z chromosome from their hemizygous F_1 mother and a Z chromosome of matching
163 subspecies identity from their father. Females have only a single Z chromosome inherited from their
164 father. Paternal backcrosses have mismatched mitochondrial and nuclear genomes, but also have a

low level of admixture on autosomes in their nuclear genome, which would otherwise be a potentially confounding source of hybrid disfunction. For this reason, we included maternal backcross individuals as controls, as their level of autosomal admixture is the same as paternal backcrosses, but their mitochondria and Z chromosomes come from the same subspecies (Figure 2). It is worth noting that these several different types of backcrossed hybrids are also highly relevant to the wild hybrid zone, where we previously described that ~68% (243 of 357) of individuals had some level of admixture[32].

The goal of our cross design was to create embryos in which the mitochondrial haplotype (i.e., mitotype) of the two subspecies was placed in three distinct contexts: 1) a nuclear genetic background exactly matching the mitotype lineage (parental crosses), 2) a nuclear genetic background that mostly did match the mitotype lineage (maternal backcrosses), and 3) a nuclear genetic background that mostly did not match the mitotype lineage (paternal backcrosses). The six resulting groups of embryos were thus 1. Parental *acuticauda* (*acuticauda* mother × *acuticauda* father), 2. Parental *hecki* (*hecki* mother × *hecki* father), 3. Maternal backcross *acuticauda* (F_1 mother with *acuticauda* mtDNA × *acuticauda* father), and 4. Maternal backcross *hecki* (F_1 mother with *hecki* mitotype × *hecki* father), 5. Paternal backcross *acuticauda* (F_1 mother with *acuticauda* mtDNA × *hecki* father), and 6. Paternal backcross *hecki* (F_1 mother with *hecki* mtDNA × *acuticauda* father). Mothers used in parental crosses only produced a single clutch while F_1 hybrid mothers used for backcrossing produced two clutches: one with a *hecki* father and one with an *acuticauda* father (however, 4 F_1 females only produced a clutch with one partner). All fathers were only used for a single clutch.

Heart rate measurement

After 12 days of incubation each egg was removed from the incubator and immediately placed on a Buddy digital egg monitor (Vetronic Services, Abbotskerswell, Devon, U.K.), to measure embryonic heart rate from within the egg (a proxy for whole body metabolic rate)[37]. A timer was started when the egg was removed from the incubator, and heart rate and corresponding time since removal were recorded at least twice over two minutes. We used these measurements to calculate the rate of cooling and the predicted heart rate halfway through the period (i.e., at 60 seconds). Five individuals where heart rate was only measured once were excluded from this dataset.

High resolution respirometry strategy

High resolution respirometry was performed with permeabilised tissue samples from these embryos using an Oroboros O2k (Oroboros Instruments, Innsbruck, Austria). High resolution respirometry allowed us to systematically stimulate, uncouple and inhibit certain combinations of mitochondrial

199 complexes (Table 3; Figure S1). We measured the maximum capacity of OXPHOS system when fuelled
200 by electrons either through both complex I, or both I and II in tandem (OXP-I, OXP-I,II), and the
201 maximum capacity of the ETS when accepting electrons from CxII, and both CxI and II in tandem (ETS-
202 I,II, ETS,II). Comparing our experimental groups for these measures reveals whether CxI is
203 compromised. We also assessed the maximum capacity for complex IV in isolation to consume O_2, a
204 measure not reliant on CxIII, which can reveal if CxIII is compromised. We assessed LEAK-I,II
205 respiration, which reflects respiration not available to fuel ATP synthesis.
206
207 These measures enable us to test whether mitonuclear interactions impact mitochondrial
208 aerobic metabolism in long-tailed finch hybrids. More specifically, they allow us to interrogate the
209 source of any mitonuclear disfunction, be it from the two complexes with amino acid differences
210 between subspecies (CxI and III) or from translational issues related to fixed differences in the mtDNA
211 encoded tRNAs or rRNAs. It is possible that some aspect of mitochondrial function other than aerobic
212 respiration is impaired, but that respiration rate is maintained. For this reason we also measured ROS-
213 induced damage. High ROS levels resulting from mitochondrial disfunction can damage
214 macromolecules, cell components and structures[38,39] and ROS-induced DNA damage correlates
215 with shorter lifespan in the closely related zebra finch[40].
216
217 **High resolution respirometry technical steps**
218 After the embryonic heart rate was measured, embryos were used for high resolution
219 respirometry. Embryos were euthanised via decapitation and then weighed (Mettler Toledo, PB303-
220 S/FACT, Colombus, Ohio, USA). There was no significant difference between experimental groups in
221 embryonic survival ($X^2_5 = 4.1$, $p = 0.53$; Figure S3B) or mass at day 12 of incubation ($X^2_5 = 7.3$, $p = 0.20$;
222 Table 3; Figure S3C). The head and body were then laterally cut in two, and the right-hand side was
223 placed in 400 µl of phosphate buffered saline (PBS), homogenized with three strokes of a teflon7-glass
224 Potter-Elvehjem homogenizer (Wheaton, 5 mL), and stored at -80 for later analyses including DNA
225 extraction for sex determination (described below). The left-hand side was weighed, suspended in a
226 dilution of 100 mg/mL of MiR05 medium (0.5 mM Egtazic Acid (EGTA), 3 mM MgCl2, 50 mM K-
227 lactobionate, 20 mM taurine, 10 mM KH2PO4, 20 mM Hepes, 110 mM sucrose, free fatty acid bovine
228 serum albumin (1 g L-1), pH 7.1;[41,42]); and then homogenized and mechanically permeabilised using
229 a teflon-glass Potter-Elvehjem homogenizer (Wheaton, 5 mL). All work was done on ice. This
230 homogenate was centrifuged for 1 min at 100 g to pellet big tissue, and then 500ul of the supernatant
231 was added to a chamber of an Oroboros O_2k high resolution respirometer set at 37°C. The
232 respirometer had two chambers and we always ran two samples in parallel. After two samples were

233 loaded and the system had equilibrated (oxygen consumption was stable), 2 µl of digitonin (10 mg/mL)
234 was added to ensure cells were fully permeabilised. We injected 5 µl pyruvate (5mM final), 5 µl malate
235 (2mM final), 10 µl glutamate (10mM final) as electron donors for CxI, and then measured oxidative
236 phosphorylation when only CxI was receiving electrons (OXPHOS-I) by adding 5 µl adenosine
237 diphosphate (ADP, 1.25 mM final). We next measured coupled respiration capacity through both CxI
238 and II (OXPHOS-I,II) by adding 25 µl succinate (10 mM final). We then determined O_2 consumption
239 associated with proton leak when electrons were being received by both CxI and II (LEAK-I,II) by adding
240 5 µl oligomycin (10 uM final). We next estimated the maximum capacity of the electron transport
241 system (ETS-I,II) by titrating the mitochondrial uncoupler carbonyl cyanide m-chlorophenyl hydrazine
242 (CCCP; at 2 mM concentration) by first one injection of 3 µl, followed by 1 µl steps. We next estimated
243 the ETS capacity when only receiving electrons through CxII (ETS-II) by adding 1 µl rotenone (0.5 uM
244 final). We then measured non-mitochondrial O2 consumption by injecting 1 µl of antimycin A (2.5 uM
245 final) to inhibit CxIII. Finally, we estimated the respiration capacity of CxIV directly by first adding 5 µl
246 TMPD (0.5 mM final) and 5 µl ascorbate (2 mM final), and then calculating the background chemical
247 respiration rate by adding 50 µl azide (100 mM final). Across all runs the chambers were opened
248 consistently at the same stages for reoxygenation. After each run 1 ml of the solution was taken from
249 each respirometer chamber and frozen at -80 ^{o}C, and at the conclusion of all measures we performed
250 a Pierce BCA protein quantification assay on this stored solution (ThermoFisher, Scientific, Waltham,
251 MA, USA). Protein quantity was included as a covariate in statistical models (below) to account for
252 slight differences in the amount of biological material in each sample. In most cases a different embryo
253 sample was run in each chamber, but in 40 cases the same embryo was run in duplicate to assess how
254 repeatable these measurements were (Table 3). When two different samples were run, the first was
255 sitting in the respirometer for some time before the protocol was begun, and to account for any
256 variability introduced by this we included a covariate in our models that was the length of time
257 between when the embryo sample entered the chamber and when the measure was made.
258
259 **Molecular sexing**
260 We extracted DNA from the homogenized right-side of all embryos using a Gentra PureGene kit
261 (Qiagen, Valencia, CA, USA) following manufacturer instructions. We sexed embryos by amplifying an
262 intronic portion of the CHD gene that differs in size between the Z-linked and W-linked copy following
263 published protocols[32,43]. Gel electrophoresis of the PCR product revealed the sex of the embryo as
264 either male (one band, homozygous, ZZ) or female (two bands, heterozygous, ZW).
265
266 **mtDNA copy number**

267 We estimated mitochondrial density based upon mtDNA copy number for all samples using real-time
268 quantitative PCR (qPCR) analysis following protocols established for passerine birds (Stier et al. 2019,
269 2022). While the amount of mtDNA in a mitochondrion can vary, mtDNA copy number is a reliable
270 proxy of mitochondrial density. We estimated the relative mtDNA copy number by measuring the
271 amount of mtDNA relative to the nuDNA for each sample by qPCR on a CFX96 Real-Time System (BIO-
272 RAD). We used RAG1 as a representative single-copy nuclear gene (F: GCAGATGAACTGGAGGCTATAA,
273 R: CAGCTGAGAAACGTGTTGATTC) and used COX1 as our representative mitochondrial gene (F:
274 TCCTAGCCAACTCCTCAC, R: CCTGCTAGGATTGCAAAT). A complete nuclear copy of the mitochondrial
275 genome (i.e., a NUMT) exists in Estrildid finches; for example, in the zebra finch reference genome
276 (GCA_003957565.4) at chr2:72232845-72249691. To minimize the risk of NUMT interference in
277 estimating mtDNA copy number, we designed our COX1 primers to perfectly match the mitochondrial
278 sequence observed in *Poephila*. Moreover, our use of embryo tissue is less likely to result in
279 amplification of the NUMT as gDNA from muscle tissue has a much lower nuclear:mitochondria ratio
280 than gDNA from blood[44]. We further verified that COX1 amplification resulted in a single product of
281 the expected size on an agarose gel.
282
283 Following Stier et al. (2022), qPCR reactions had a total volume of 12 µl that included 6 ng of
284 DNA, had PCR primers with concentrations of 200 nM and 6 µl of Absolute Blue qPCR Mix SYBR Green
285 low ROX (Thermos Scientific). The qPCR conditions were: 15 mins at 95°C, 40 cycles of 15 s at 95°C, 30
286 s at 58°C, 30 s at 72°C. Samples were run in triplicate for each gene (RAG1 and COX1) across 5 plates,
287 ten samples were pooled and included on every plate as a reference, and 20 samples were included
288 on two separate plates. Amplicon efficiency was estimated from a standard curve of the reference
289 between 1.5 to 24 ng (1.5, 3, 6, 12, 16, 24) run on one plate. The mean reaction efficiencies were
290 92.1% for RAG1 and 82.3% for COX1. To calculate relative mtDNA copy number for each sample we
291 used the following formula: $(1+Ef_{COX1})^{\Delta CqCOX1}/(1+Ef_{RAG1})^{\Delta CqRAG1}$, with Ef as the amplicon efficiency, ΔCq
292 as the difference in Cq between the reference and focal samples. Some samples were run twice on
293 separate plates, with an inter-plate repeatability of 0.74 (95% C.I. [0.49, 0.88]), and based on triplicates
294 intra-plate repeatability was 0.94 (95% C.I. [0.93, 0.95]). Seven samples were considered as outliers
295 (Cq RAG1 < Cq COI) and removed from analysis.
296
297 **Oxidative Damage assay**
298 8-OHdG (8-hydroxy-2'-deoxyguanosine) is a predominant form of ROS-induced oxidative lesion that
299 has been widely used as a biomarker for oxidative damage[45], including alongside measures of
300 respiration capacity in birds[46,47]. Here we quantified levels of 8-OHdG in the DNA extracted from

301 embryos using a competitive immunoassay (300 ng DNA, EpiQuick 8-OHdG DNA Damage
302 Quantification Direct Kit Colorimetric, Epigentek, USA) following the manufacturer recommendations.
303 This was run on a subset of samples (N = 182) chosen blind to respiration capacity to have roughly
304 balanced numbers from each experimental group (N = 28-33 samples per group). The intra-plate
305 coefficient of variation based on duplicates was 6.3 $\pm$ 0.83. The inter-plate coefficient of variation
306 based on four samples repeated over all three plates was 22.7 $\pm$ 4.05, so we included plate ID as
307 random effect in our analyses.
308
309 **Statistical analyses**
310 For statistical analyses we used R version 4.1.2 (R Core Team 2020) using RStudio version 1.2.5033
311 (RStudio Team, 2020) for the graphical interface. We used the lme4 and lmerTest packages[53,54] to
312 run linear mixed models to test whether our measures of respiration capacity differed between the
313 six experimental groups (parental *acuticauda*, parental *hecki*, maternal and paternal backcross with
314 acuticauda mtDNA, maternal and paternal backcrosses with hecki mtDNA). These measures were each
315 included as the dependent variable in separate linear mixed models, in which the fixed effects were
316 experimental group, embryo sex, protein quantity in the chamber, and the length of time after embryo
317 entered the oroboros chamber when the measure was made. In each we tested for an interaction
318 between experimental group and embryo sex, and if this was not significant the interaction term was
319 removed (but left in the model if significant). In each model parental pair ID was included as a random
320 effect, to account for multiple members of the same clutch being included. Where there was a
321 significant effect of experimental group, we ran Tukey post-hoc comparisons using the emmeans
322 package[55] to assess specifically which groups differed from one another. Model assumptions were
323 checked using the DHARMa package in R[56].
324
325 We similarly ran linear mixed models to test whether heart rate, oxidative damage and
326 mitochondrial copy number differed between our experimental groups, but in these cases the fixed
327 effects were experimental group, embryo sex, and for the heart rate model embryo mass, and the
328 random effect was still parental pair ID. Oxidative damage and mitochondrial copy number were log-
329 transformed to better meet model assumptions. An interaction between experimental group and sex
330 was also included for each model, but then removed if not significant. In the mitochondrial copy
331 number and oxidative damage models, plate ID were additionally included as random effects. Embryo
332 ID was also initially included as a random effect in the mitochondrial copy number and oxidative
333 damage models, but it explained close to zero variance so was removed for the final models, likely
334 because very few individuals were measured twice (10 for mitochondrial copy number, 21 for

335 oxidative damage). A small number of values for mitochondrial copy number were extremely high (N
336 = 10, total N = 211), well above the normally distributed other samples and were likely technical errors,
337 and so were excluded to facilitate modelling. When plotted they were distributed roughly evenly
338 between experimental groups so their inclusion would be unlikely to change the results anyway.
339

340 **Results**

341

342 We found a low level of divergence in mtDNA between subspecies, with fixed differences observed in
343 only 0.9% of positions comprising the protein-coding genes of the electron transport system (107 of
344 11,361 bp total; Table 1). Absolute divergence (D_{XY}) was highly variable, however, across protein-
345 coding genes, ranging from 0% (ATP8) to 3.3% (NAD6), and between complexes: divergence was 2.1-
346 fold higher on average for genes in complex I than in complex IV (Table 1). We observed a total of
347 seven fixed amino acid differences between subspecies, five differences in four genes in complex I,
348 and two amino acid differences in the cytochrome b (COB) gene in complex III. There were no amino
349 acid differences between the subspecies in either complex IV or complex V. The inferred mitochondrial
350 genome-wide dN/dS ratio between long-tailed finch subspecies is well below 1 at 0.0168, suggesting
351 that purifying selection is the dominant force shaping mitochondrial evolution in *Poephila* (Table 1).
352 Of the five genes with observed non-synonymous differences between subspecies, dN/dS ranged from
353 0.0127 (*NAD5*) to 0.1142 (*NAD3*).
354

355 In the non-coding region, we observed a further six fixed differences between subspecies in
356 the small and large rRNA genes (four and two differences, respectively) and a total of four fixed
357 differences in four mitochondrial tRNAs (Table S1). These non-coding differences provide additional
358 potential sites of mitonuclear incompatibilities that could impact mitochondrial function via the
359 transcription, translation, or replication of mtDNA [e.g., 41]. On the other hand, any protein-protein
360 mitonuclear incompatibilities in this system should be restricted to impacting the function of
361 complexes I or III.
362

363 Polarization inference from the use of outgroup taxa revealed that of the seven fixed amino
364 acid differences between subspecies, six have occurred in the *hecki* lineage (Figure 3; Table 2). Three
365 of the amino acid substitutions derived within *hecki*, and the single amino acid change derived in
366 *acuticauda*, result in a change from a polar to a non-polar amino acid (Table 2). In the non-protein
367 coding genes (rRNAs, tRNAs, OH) there was a roughly even spread of derived DNA sequence changes
368 between lineages (6 *acuticauda* and 4 *hecki,* Table S1 and S3).
369

370 We observed a significant difference between the two paternal backcross groups for all five
371 measures of aerobic respiration capacity (except borderline non-significant for females for OXP-I,II, p
372 = 0.064), whereby individuals with *acuticauda* mtDNA and *hecki* nuDNA had lower respiration capacity
373 than did individuals with *hecki* mtDNA and *acuticauda* nuDNA (Table 3; Figure 4, Figure S2). There
374 were no other differences between experimental groups that were as consistent across the five
375 measures of aerobic capacity we measured (Table 3). For the measure ETS-I,II the paternal backcross
376 *hecki* mitotype was significantly higher than the maternal backcross *acuticauda* mitotype, and for
377 OXP-I females the parental group *hecki* was significantly higher than the paternal backcross
378 *acuticauda* mitotype group (Table 3).
379
380 We did not find a difference between groups in oxidative damage (Table 3, Figure S3D). We
381 also found no evidence that this difference in aerobic respiration capacity between paternal backcross
382 groups was driven by different quantities of mitochondria per cell, with the relative mtDNA copy
383 number not significantly differing between the two paternal backcross groups, or between them and
384 other groups (Table 3) and so likely not driving the aerobic respiration capacity results. We also found
385 no difference between experimental groups in heart rate on day 12 of incubation immediately after
386 being removed from the incubator and so no evidence that whole body metabolism is impacted by
387 hybrid cross (Table 2, Figure S3C).
388

389 ## Discussion

390

391 We found evidence that an interaction between the mitochondrial and nuclear genomes of long-tailed
392 finch subspecies impacted aerobic respiration capacity in hybrids, despite the low level of divergence
393 in mtDNA between them (<1%). These observations identifying the effect of mitonuclear
394 incompatibilities on aerobic respiration have important implications for both mtDNA introgression
395 and reproductive isolation in the long-tailed finch system. Positive selection can drive allelic
396 introgression across a hybrid zone, as can neutral processes (such as range expansion). In the long-
397 tailed finch hybrid zone there are high levels of admixture (~68% of individuals have some degree of
398 mitonuclear mismatch), and so selection will be acting on each mitotype in several different nuclear
399 contexts, akin to those generated through our experimental approach. Our primary result suggests
400 that there is no difference in mitochondrial aerobic metabolism between the mitotypes in the pure
401 parental context or in the maternal backcross individuals, but that the *acuticauda* mitotype has
402 reduced respiration capacity in the paternal backcross context compared to the *hecki* mitotype in the
403 paternal backcross context. In the regime of widespread admixture within the hybrid zone, negative

404 selection on the *acuticauda* mitotype might result in the *hecki* mitotype increasing in frequency and
405 introgressing westwards. This is indeed what is observed in the wild long-tailed finch hybrid zone,
406 where the centre of the mitochondrial cline is displaced 55 km west of the nuclear cline centre (Figure
407 1B & C). Respiration capacity reflects the upper limit of mitochondrial aerobic respiration. Therefore,
408 the reduced aerobic capacity observed for *acuticauda* mtDNA paternal backcross individuals is
409 expected to be detrimental, particularly for energetically demanding tissues and life-stages. This
410 suggests that the physiological effects observed in this experiment may be a good proxy for the
411 selection that is occurring in the wild.
412
413 We did not, however, find strong evidence that mitonuclear incompatibilities reduce hybrid
414 fitness compared to parental individuals. There were few differences between our paternal backcross
415 groups and either pure parental individuals or maternal backcross groups (Table 3; Figure 4; Figure
416 S2). A conservative interpretation would suggest that incompatibilities between the mitochondrial
417 and nuclear genomes of these subspecies is not a key component of reproductive isolation between
418 them, which might instead be linked to other incompatibilities such as those involving chromosomal
419 inversions [31]. Our lack of difference between parental and paternal backcross groups are in stark
420 contrast to results from comparable experiments using deeply diverged lineages crossed in the lab
421 (e.g., with mitochondrial divergence >10%), where paternal backcrossed individuals had dramatically
422 impacted mitochondrial function, survival, or fecundity [13,14,62,63]. There are however some lines
423 of evidence suggestive of nascent mitonuclear incompatibility in this study. For a few respiration
424 measures, there were significant – or borderline significant – differences between paternal backcross
425 and maternal backcross groups; for ETSI,II (Figure 4) and ETS-II *hecki* paternal backcrosses had higher
426 respiration capacity than did *acuticauda* maternal backcrosses, and for CxIV the *acuticauda* paternal
427 backcrosses had borderline significantly lower respiration capacity than *hecki* maternal backcrosses
428 (Table 3; Figure S2). Furthermore, while not statistically significant, the mean respiration values of
429 both paternal backcross groups were shifted away from the parental groups, which may reflect
430 divergence from the species-specific optima. It is possible that we may simply not have had enough
431 statistical power to detect weak effects. Mitonuclear disfunction may only become apparent in
432 specific tissue types with high baseline energy consumption (e.g., cardiac or nervous system tissue) or
433 under stressful conditions with heightened energetic demands (e.g., during reproduction or thermal
434 stress). Thus, our observations do not preclude a role for mitonuclear incompatibilities as a
435 reproductive isolating barrier at this early stage of population divergence.
436

437 We were interested in distinguishing what mitonuclear components were likely interacting to
438 impact mitochondrial aerobic respiration. We wanted to know whether the observed differences in
439 aerobic respiration between paternal backcross groups was the result of specific protein-protein
440 interactions in complexes I and III or if instead they were due to interactions involving mtDNA encoded
441 tRNA or rRNA. The difference between the two paternal backcross groups was consistent across all
442 measures, which included the CxIV respiration measure that is not dependent on other complexes
443 and there are no fixed differences in CxIV amino acids between subspecies. This suggests that the
444 causal mitonuclear interaction may not be between proteins encoded by the two genomes but may
445 instead be between either mtDNA encoded tRNA and nuDNA encoded aminoacyl tRNA synthetases,
446 or between mtDNA encoded rRNA and nuDNA encoded ribosomal proteins. These interactions would
447 impact the translation of mtDNA and therefore the production of all mtDNA encoded ETS complexes
448 (CxI, III, IV, and V).
449
450 There was also a significant sex difference in the *hecki* subspecies for two measures (OXP-I,II
451 and OXP-I), whereby females had higher respiration capacity than males (Table 3; Figure S2). As a
452 result, female parental *hecki* individuals had higher respiration capacity than *acuticauda* mtDNA
453 parental backcross individuals, and male parental *hecki* individuals had lower respiration capacity than
454 did *hecki* mtDNA parental backcross individuals. It is unclear to us why there is a sex difference in
455 respiration capacity for *hecki* individuals but not *acuticauda* or backcrossed individuals. This may just
456 be a false positive, as we have run many statistical tests in this study, but it may be biological; sex
457 differences in mitochondrial function have been observed in the literature, although there is no
458 apparent consistent difference[64]. Furthermore, as embryos we would not expect dramatic sex
459 differences in metabolism, except perhaps the gonads. 'Mother's curse' is a phenomenon that can
460 result in a sex effect due to mitonuclear interactions[65–67], but it predicts that detrimental impacts
461 of mtDNA on males and resulting sex differences are exposed with heterospecific nuDNA but not
462 homospecific nuDNA (due to nuDNA coevolution to rescue function), whereas in the present study we
463 found the opposite; that seemingly detrimental impacts of mtDNA only occurs in homo(sub)specific
464 nuDNA context.
465
466 We did not find evidence that the observed effects on cellular aerobic respiration capacity
467 between paternal backcross groups affected our proxies for whole-organism metabolic rate or the
468 level of oxidative damage. The inter-lineage mitonuclear interactions may therefore be impacting
469 fitness through other pathways or under specific circumstances, for example in energetically
470 demanding tissues and life-stages. Given the experimental context it would also be valuable to confirm

471 the whole-body result with more direct measures of metabolism (e.g., open-flow respirometry[68]).
472 This is because other differences between experimental groups may undermine how well heart rate
473 reflects differences in whole-body metabolism, for example at low incubation temperature, Japanese
474 quail heart rate decreases[69] but heart volume increases to compensate (A. Stier, unpublished data).
475
476 Purifying selection appears to be the dominant force in mtDNA evolution in *Poephila* (the
477 mitochondrial genome-wide dN/dS ratio is well below 1 at 0.0168). The observed amino acid
478 differences between long-tailed finch subspecies are thus notable, with all six *hecki*-derived amino
479 acid changes are in genes within complexes I (four AAs) and III (two AAs) suggesting some degree of
480 inter-molecular epistasis might exist between these substitutions. Moreover, in one of the genes with
481 multiple non-synonymous substitutions (COB), amino acid changes were located <15 codon positions
482 apart, a possible signature of intra-molecular epistasis [57,58]. Taken together this may constitute
483 evidence of adaptive evolution within *hecki*, as mitochondria can contribute to local adaptation (e.g.,
484 to differences in climate)[59–61], but to confirm this requires further investigation.
485
486 In conclusion, we here demonstrate that functional consequences of interactions between
487 mtDNA and nuDNA are possible even at a low level of divergence (<1% mtDNA), and the resulting
488 impact on fitness between the two groups with mitonuclear mismatch in this system may be strong
489 enough to result in asymmetrical mitochondrial introgression across a hybrid zone. Such mitonuclear
490 interactions may be widespread, as most avian lineages with stable hybrid zones have equal or greater
491 divergence. Researchers considering cases of mitonuclear discordance (or cyto-nuclear discordance
492 more generally) should consider that functional consequences of mitonuclear interactions may be at
493 play[23,70]. Identifying the specific genes involved in mitonuclear interactions in the long-tailed finch
494 would be a valuable direction for future research, as this will facilitate testing the molecular pathways
495 involved in mitonuclear interactions and the evolutionary processes that led to them (e.g., rapid
496 evolution)[20,63,71–74]. This sensitivity of mitochondrial function to genetic variation, their centrality
497 to organismal function (generating 90% of cellular energy in animals[75]), and the broad range of taxa
498 that rely on mitochondria for energy production support suggestions that mitonuclear interactions
499 may be a powerful force acting on hybridising animals[76–79].

Ethics statement

This experiment was approved by the Macquarie University Animal Ethics Committee (reference number: 2020/021) and all experiments conform to the relevant regulatory standards.

Funding

This work was supported by an Australian Research Council (ARC) Discovery Project to SCG and DMH (DP180101783), and a Holsworth Wildlife Research Endowment from Equity Trustees Charitable Foundation and the Ecological Society of Australia and a Macquarie University Research Excellence Scholarship to CSM. AS was supported by a 'Turku Collegium for Science and Medicine' Fellowship and a Marie Sklodowska-Curie Postdoctoral Fellowship (#894963). Gerstner Scholars Fellowship and the Gerstner Family Foundation, and the Richard Gilder Graduate School at the American Museum of Natural History provided support to DMH.

Data Accessibility and Benefit Sharing

Data from the respiration capacity, oxidative damage, heart rate and mitochondrial copy number, the R scripts for statistical analyses are available on the Open Science Framework (https://osf.io/f652p/?view_only=30142041d5d74dd7bd904ddac0186a41). Mitochondrial sequences for this project will be deposited in GenBank's nucleotide archive at time of publication. The WGS data used to assemble mitogenomes is part of another study currently in prep and will be made available when that work is published.

Acknowledgements

The authors would like to thank Riccardo Ton and Hector Pacheco Fuentes for providing assistance setting up the Oroboros O_2k, and Macquarie Animal Research Services (M.A.R.S.) staff for providing daily bird husbandry.

Competing interests

The authors declare no competing interests.

Author contributions

Conceptualization, C.S.M., S.C.G.; Methodology, C.S.M., D.M.H., A.S., S.C.G; Investigation, C.S.M.; Data analysis and interpretation, C.S.M., D.M.H., A.S.; Resources, S.C.G.; Writing – Original Draft, C.S.M.; Writing – Review & Editing, C.S.M, D.M.H., A.S., S.C.G.; Visualization, C.S.M., D.M.H.; Supervision, S.C.G.; Funding Acquisition, C.S.M., D.M.H., S.C.G.

534 **Table 1 | Mitochondrial protein-coding divergence between long-tailed finch subspecies**. The 13
535 protein-coding genes comprising the electron transport system (ETS) are organized by complex. Fixed
536 differences between subspecies were inferred based on comparison of full mitochondrial genomes of
537 *Poephila a. acuticauda* (N = 14) and *P. a. hecki* (N = 11) with D_{XY} calculated as the absolute divergence
538 between members of each subspecies. Estimates of dN/dS were calculated for each gene using the
539 model M0 implemented in the program Easy-CodeML (v1.41; Gao et al 2019). The combined estimate
540 of dN/dS was inferred based on net dN (0.0114) and dS (0.6802) across all protein-coding genes.
541

Complex	Gene	Fixed differences	D_{XY}	dN/dS
Complex I	*NAD1*	12	0.012	0.0001
	NAD2	8	0.008	0.0001
	NAD3	3	0.009	0.1142
	NAD4	9	0.007	0.0599
	NAD4L	5	0.017	0.0001
	NAD5	17	0.009	0.0127
	NAD6	17	0.033	0.0210
Complex III	*COB*	10	0.009	0.0574
Complex IV	*COX1*	9	0.006	0.0001
	COX2	4	0.006	0.0001
	COX3	3	0.004	0.0001
Complex V	*ATP6*	10	0.015	0.0001
	ATP8	0	0.000	0.0001
	Combined	**107**	**0.009**	**0.0168**

542

543 **Table 2 | mtDNA amino acid differences between long-tailed finch subspecies**. Fixed differences
544 were assigned to their lineage of origin using mitochondrial genomes of the black-throated finch
545 (*Poephila cincta atropygialis*; N = 11) and the zebra finch (*Taeniopygia guttata*; N = 1) as outgroups.
546

Complex	Gene	Mutation	Biochemical Change	Origin
Complex I	*NAD3*	T9A	polarity change (+ > -)	*hecki*
	NAD4	T96A	polarity change (+ > -)	*hecki*
	NAD4	T398A	polarity change (+ > -)	*hecki*
	NAD5	A16V	none	*hecki*
	NAD6	S127L	polarity change (+ > -)	*acuticauda*
Complex III	*COB*	S358T	none	*hecki*
	COB	I372M	none	*hecki*

547

Table 3 | Model output comparing the measures of mitochondrial function and physiology measures among the six experimental groups.

Respiration measure	ETS Cxs included	Description of measure	Repeatability (SE) from 40 samples run in duplicate	Cross*Sex	Sex (if split model due to interaction)	Cross	Sex	Protein Qty	Length of time	Var.	MargR²	ICC Pair ID	CondR²	G5<G6	G6>G3	G2<G6	G2>G5	G5<G4
				X2 (DF) p-value		X2 (DF) p-value	X2 (DF) p-value	X2 (DF) p-value	X2 (DF) p-value					Showing p-values for p < 0.1.				
OXP-I,II	I,II,III,IV,V	Coupled respiration	0.94 (0.02)	**11.5 (5) 0.043**	Female	**12.73 (5) 0.026**	NA	2.59 (1) 0.11	**8.68 (1) 0.003**	197	0.62	0.37	0.99	*0.064*			*0.072*	
					Male	**13.87 (5) 0.016**	NA	**7.98 (1) 0.005**	**9.31 (1) 0.002**	240	0.44	0.55	0.99	**0.042**		*0.093*		
ETS-I,II	I,II,III,IV	Uncoupled respiration	0.90 (0.03)	9.78 (5) 0.08		**20.15 (5) 0.001**	2.3 (1) 0.13	**4.06 (1) 0.044**	**26.1 (1) <0.001**	289	0.53	0.46	0.99	**<0.001**	**0.034**			
OXP-I	I,III,IV,V	Coupled respiration	0.69 (0.09)	**11.97 (5) 0.035**	Female	**15.4 (5) 0.009**	NA	*3.29 (1) 0.07*	**25.2 (1) <0.001**	206	0.79	0.20	0.99	**0.029**			**0.036**	
					Male	**14.9 (5) 0.010**	NA	**6.67 (1) 0.010**	**33.11 (1) <0.001**	224	0.63	0.36	0.99	**0.030**		*0.052*		
ETS-II	II,III,IV	Maximum capacity of the ETS	0.96 (0.01)	7.1 (5) 0.2		**19.6 (5) 0.002**	1.53 (1) 0.22	**5.04 (1) 0.02**	1.17 (1) 0.28	55	0.39	0.58	0.98	**0.001**	*0.065*			
CxIV	IV	Maximum respiration	0.93 (0.02)	8.7 (5) 0.12		**19.8 (5) 0.001**	1.5 (1) 0.22	**7.8 (1) 0.005**	2.14 (1) 0.14	302	0.41	0.58	0.99	**0.001**				*0.056*
LEAK-I,II	I,II,III,IV	Respiration linked to proton leak	0.89 (0.03)	*9.6 (5) 0.09*		**17.3 (5) 0.004**	2.4 (1) 0.12	**8.6 (1) 0.003**	0.3 (1) 0.58	1.4	0.19	0.36	0.55	**0.003**				
Measure				Cross*Sex	Sex (if split model due to interaction)	Cross	Sex	Embryo Mass		Var.	MargR²	ICC Pair ID	CondR²					
Embryo Mass				8.6 (5) 0.13		7.3 (5) 0.20	0.01 (1) 0.92	NA		<0.001	<0.001	<0.001	<0.001					
Embryo Survival				NA		4.1 (5) 0.53	NA	NA		0.09	0.02	0.24	0.27					
Heart rate (proxy for whole body metabolism)				15.2 (5) 0.01	Male	7.8 (5) 0.17	NA	**23.5 (1) <0.01**		156	0.41	0.59	0.99					
					Female	6.3 (5) 0.28	NA	**8.3 (1) 0.004**		78	0.20	0.80	0.99					
Oxidative DNA oxidative damage (log transformed)				8.3 (5) 0.14		8.6 (5) 0.12	*3.0 (1) 0.08*	NA	ICC Plate: 0.008	0.019	0.006	0.012	0.026					
mtDNA copy number (log transformed)				2.2 (5) 0.82		**20.9 (5) <0.001**	0.17 (1) 0.69	NA	ICC Plate: 0.00	0.03	0.01	0.02	0.03	G5<G6 **0.005**	G1<G6 *0.093*	G3<G6 *0.090*		

Groups same as that in Figure 4. Group 1; parental group *acuticauda*, Group 2: parental group *hecki*, Group 3: maternal backcross *acuticauda* mitotype, Group 4: maternal backcross *hecki* mitotype, Group 5: paternal backcross *acuticauda* mitotype, Group 6: paternal backcross *hecki* mitotype.

Var. - variance, $MargR^2$ – marginal R^2 , ICC Pair ID – intra-class correlation coefficient value for Pair ID as a random effect, $CondR^2$ – conditional R^2.

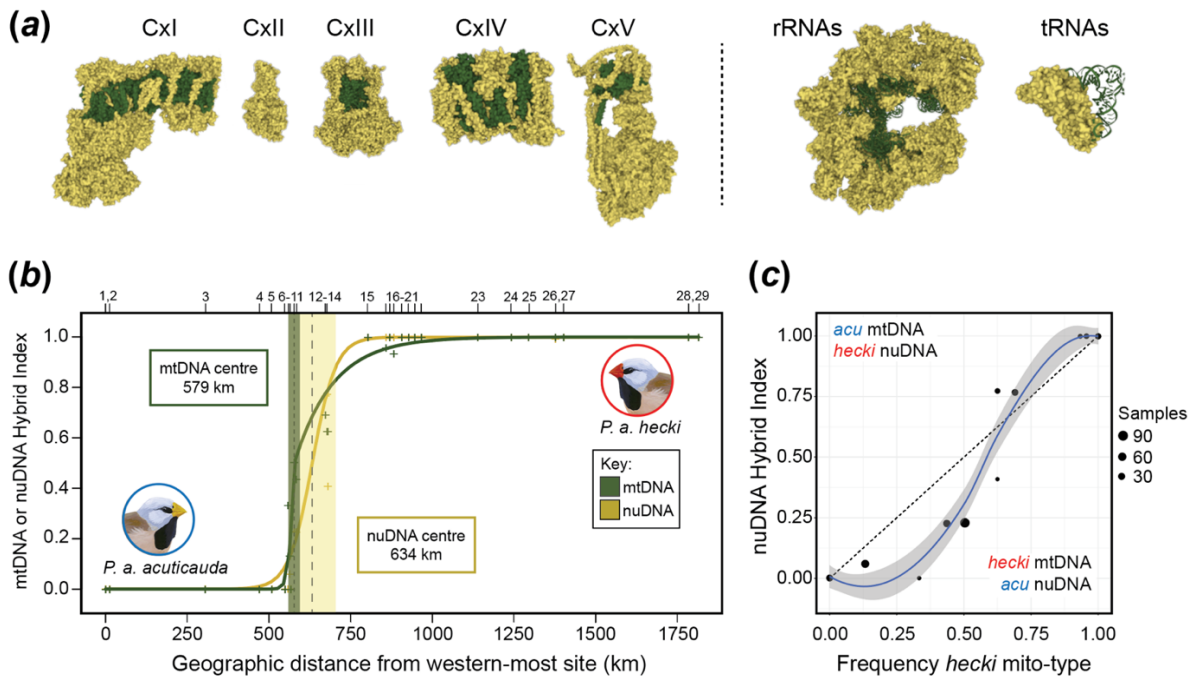

Figure 1 | Mitochondrial and nuclear genome interactions in the long-tailed finch. (*a*) Sites of physical interaction within the inner mitochondrial membrane between products encoded by the mitochondrial (green) and nuclear (yellow) genomes. These include proteins that form the electron transport system complexes (CxI-IV) and ATP synthase (CxV), as well as mitochondrial ribosomes and transfer RNA-tRNA sythetases. Complexes are not drawn to scale. The animals and PBD accession numbers for each are CxI (bovine, 5LNK), CxII (chicken, 2H89), CxIII (chicken, 3CWB), CxIV (bovine, 1V45), CxV (bovine, 5ARA – TBC), tRNA (yeast, 4YYE), rRNA (humans, 3J9M). Figure inspired by Hill et al. 2019. **(*b*)** Geographic clines for mtDNA and nuDNA (Z-chromosome) across the range of the long-tailed finch. The mtDNA cline centre is 55 km west of the nuDNA cline centre. The position of 29 sampled populations are shown above the panel and population means for mtDNA and nuDNA are presented as green or yellow crosses, respectively. **(*c*)** The frequency of the *hecki* mito-type against nuDNA hybrid index for 11 populations sampled within the hybrid zone, with a loess curve with 95% CI fitted to the data against a dashed line showing the 1:1 neutral expectation. (***b***) and (***c***) are based on re-evaluated and re-plotted published data from Lopez et al. 2021.

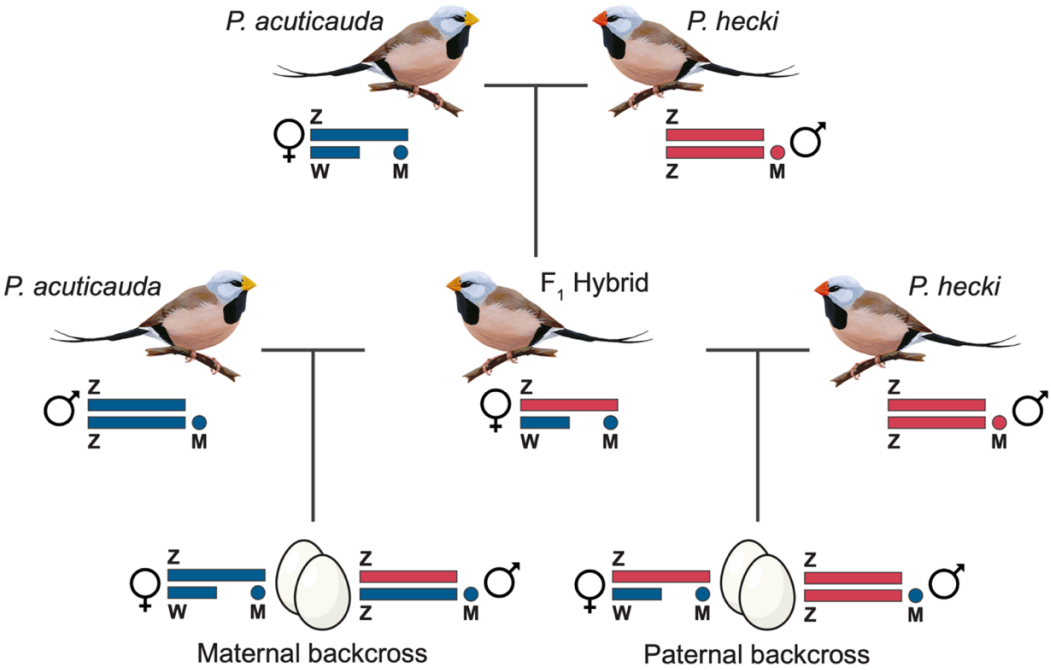

Figure 2 | Experimental design used to breed paternal and maternal backcross offspring. The example shown represents the cross between *P. a. acuticauda* females and *P. a. hecki* males used to generate maternal and paternal backcross hybrids carrying *acuticauda* mito-types. The reciprocal cross used to generate *hecki* mito-type carrying backcross hybrids was structured in the same way.

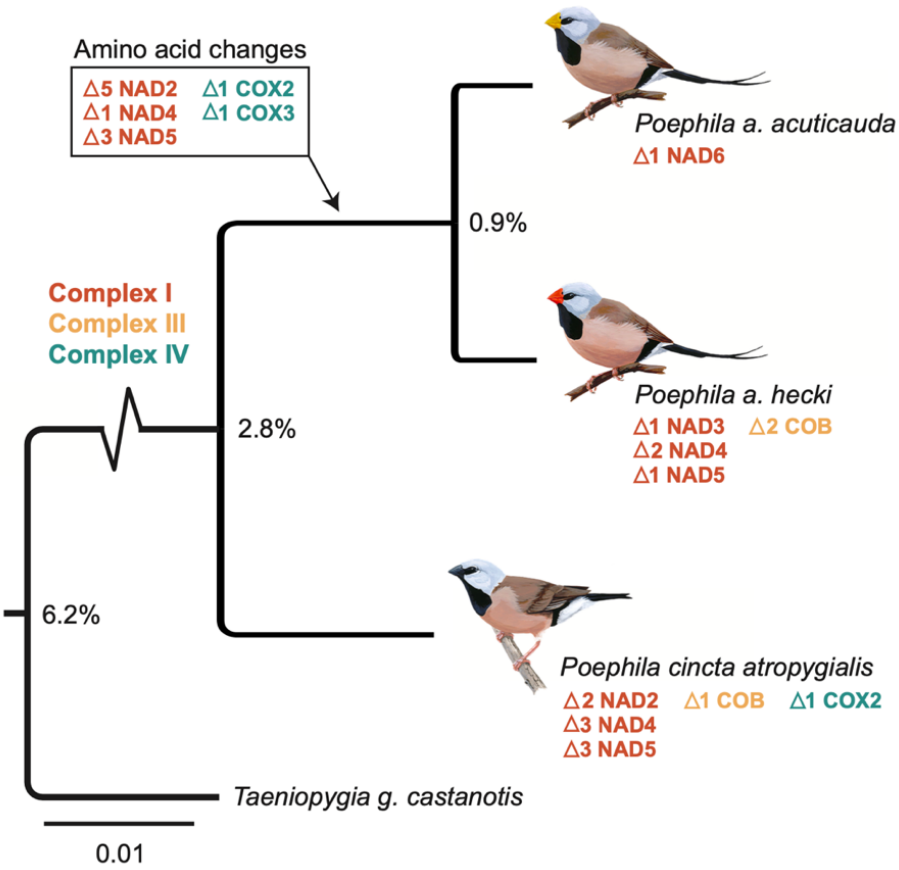

Figure 3 | Evolutionary history of mtDNA protein-coding divergence between long-tailed finch subspecies. A maximum likelihood tree was generated based on an aligned concatenation of consensus sequences for all 13 protein-coding genes using W-IQ-TREE [1] under the best-fit substitution model: TPM2u+F+I. The zebra finch (NCBI accession: DQ422742) and black-throated finch samples were used to assign all nucleotide substitutions and any associated amino acid changes to their branch of origin. Branch lengths are proportional to the number of substitutions. Divergence estimates at each node represent the total number of fixed differences between species in protein-coding genes divided by the total number of protein-coding bases (Table S2). The number of amino acid changes identified within each gene are color-coded by ETS complex: red for complex I, yellow for complex III, and blue-green for complex IV.

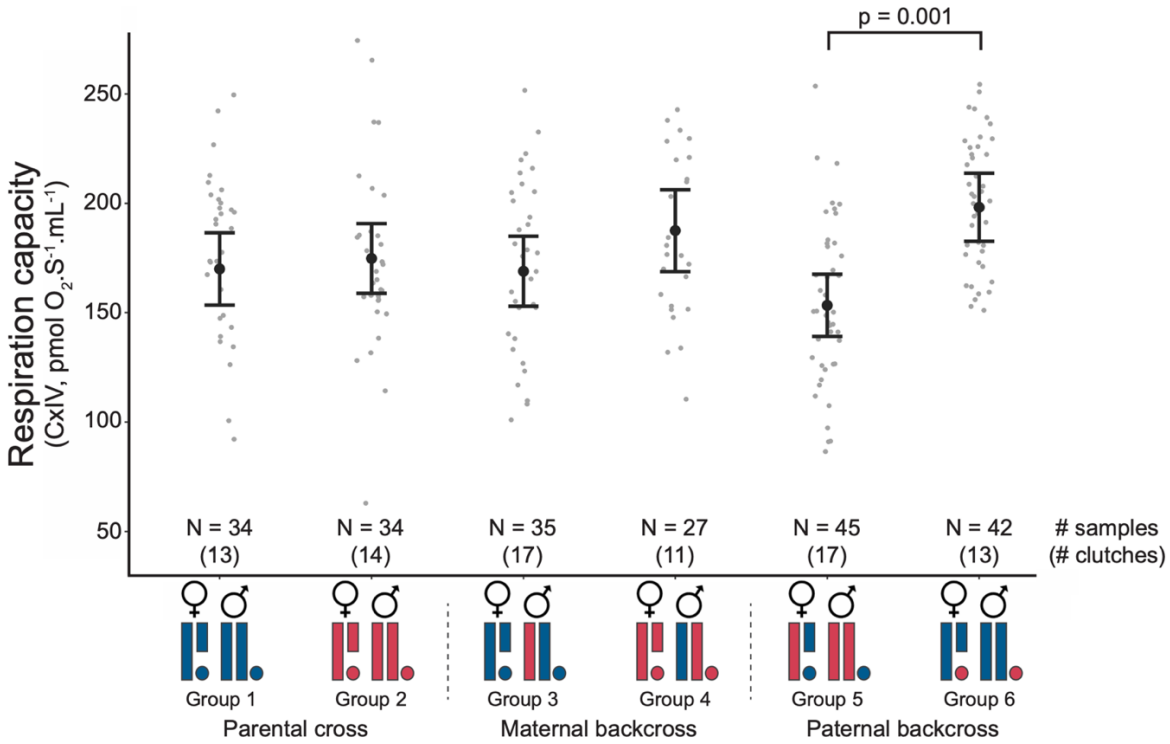

Figure 4 | Mitochondrial and nuclear genomes between the long-tailed finch subspecies interact to impact mitochondrial respiration capacity. The respiration capacity of our experimental groups, with grey datapoints indicating raw data (corrected for amount of protein), and black mean and 95% CIs reflect model output (accounting for clutch ID, protein quantity, length of time in chamber, sex). Most measures of mitochondrial respiration capacity had this same pattern of differences among the groups (Table 3; Figure S2).

599 **References**:
600

601 1. Coyne JA, Orr HA. 2004 *Speciation*. Sinauer Associates.

602 2. Chou J, Leu J. 2010 Speciation through cytonuclear incompatibility: Insights from yeast and
603 implications for higher eukaryotes. *BioEssays* **32**, 401–411. (doi:10.1002/bies.200900162)

604 3. Bar-Yaacov D, Hadjivasiliou Z, Levin L, Barshad G, Zarivach R, Bouskila A, Mishmar D. 2015
605 Mitochondrial Involvement in Vertebrate Speciation? The Case of Mito-nuclear Genetic Divergence
606 in Chameleons. *Genome Biology and Evolution* **7**, 3322–3336. (doi:10.1093/gbe/evv226)

607 4. Hill GE. 2017 The mitonuclear compatibility species concept. *The Auk* **134**, 393–409.
608 (doi:10.1642/auk-16-201.1)

609 5. Bar-Yaacov D, Blumberg A, Mishmar D. 2012 Mitochondrial-nuclear co-evolution and its effects on
610 OXPHOS activity and regulation. *Biochimica Et Biophysica Acta Bba - Gene Regul Mech* **1819**, 1107–
611 1111. (doi:10.1016/j.bbagrm.2011.10.008)

612 6. Hill GE. 2020 Mitonuclear Compensatory Coevolution. *Trends in Genetics* **36**, 403–414.
613 (doi:10.1016/j.tig.2020.03.002)

614 7. Hill. 2019 *Mitonuclear ecology*. Oxford University Press.

615 8. Allio R, Donega S, Galtier N, Nabholz B. 2017 Large Variation in the Ratio of Mitochondrial to
616 Nuclear Mutation Rate across Animals: Implications for Genetic Diversity and the Use of
617 Mitochondrial DNA as a Molecular Marker. *Mol. Biol. Evol.* **34**, 2762–2772.
618 (doi:10.1093/molbev/msx197)

619 9. Willett CS. 2012 Quantifying the Elevation of Mitochondrial DNA Evolutionary Substitution Rates
620 Over Nuclear Rates in the Intertidal Copepod Tigriopus californicus. *J. Mol. Evol.* **74**, 310–318.
621 (doi:10.1007/s00239-012-9508-1)

622 10. Nabholz B, Glémin S, Galtier N. 2008 Strong Variations of Mitochondrial Mutation Rate across
623 Mammals—the Longevity Hypothesis. *Mol. Biol. Evol.* **25**, 120–130. (doi:10.1093/molbev/msm248)

624 11. Nabholz B, Glémin S, Galtier N. 2009 The erratic mitochondrial clock: variations of mutation rate,
625 not population size, affect mtDNA diversity across birds and mammals. *BMC Evol. Biol.* **9**, 54.
626 (doi:10.1186/1471-2148-9-54)

627 12. Mower JP, Touzet P, Gummow JS, Delph LF, Palmer JD. 2007 Extensive variation in synonymous
628 substitution rates in mitochondrial genes of seed plants. *BMC Evol. Biol.* **7**, 135. (doi:10.1186/1471-
629 2148-7-135)

630 13. Ellison CK, Burton RS. 2008 Interpopulation hybrid breakdown maps to the mitochondrial
631 genome. *Evolution* **62**, 631–638. (doi:10.1111/j.1558-5646.2007.00305.x)

632 14. Ellison CK, Niehuis O, Gadau J. 2008 Hybrid breakdown and mitochondrial dysfunction in hybrids
633 of Nasonia parasitoid wasps. *J Evolution Biol* **21**, 1844–1851. (doi:10.1111/j.1420-
634 9101.2008.01608.x)

635 15. Montooth KL, Meiklejohn CD, Abt DN, Rand DM. 2010 Mitochondrial-nuclear epistasis affects
636 fitness within species but does not contribute to fixed incompatibilities between species of
637 Drosophila. *Evolution* **64**, 3364–3379. (doi:10.1111/j.1558-5646.2010.01077.x)

638 16. Arnqvist G, Dowling DK, Eady P, Gay L, Tregenza T, Tuda M, Hosken DJ. 2010 Genetic architecture
639 of metabolic rate: environment specific epistasis between mitochondrial and nuclear genes in an
640 insect. *Evolution* **64**, 3354–3363. (doi:10.1111/j.1558-5646.2010.01135.x)

641 17. Burton RS, Pereira RJ, Barreto FS. 2013 Cytonuclear Genomic Interactions and Hybrid
642 Breakdown. *Annu Rev Ecol Evol Syst* **44**, 281–302. (doi:10.1146/annurev-ecolsys-110512-135758)

643 18. Lee H-Y, Chou J-Y, Cheong L, Chang N-H, Yang S-Y, Leu J-Y. 2008 Incompatibility of Nuclear and
644 Mitochondrial Genomes Causes Hybrid Sterility between Two Yeast Species. *Cell* **135**, 1065–1073.
645 (doi:10.1016/j.cell.2008.10.047)

646 19. Ma H *et al.* 2016 Incompatibility between Nuclear and Mitochondrial Genomes Contributes to an
647 Interspecies Reproductive Barrier. *Cell Metab* **24**, 283–294. (doi:10.1016/j.cmet.2016.06.012)

648 20. Moran B *et al.* 2022 A Lethal Genetic Incompatibility between Naturally Hybridizing Species in
649 Mitochondrial Complex I. , 1–45.

650 21. Toews DPL, Mandic M, Richards JG, Irwin DE. 2014 Migration, mitochondria, and the yellow-
651 rumped warbler. *Evolution* , 1–16. (doi:10.5061/dryad.99db2)

652 22. Morales HE, Pavlova A, Amos N, Major R, Kilian A, Greening C, Sunnucks P. 2018 Concordant
653 divergence of mitogenomes and a mitonuclear gene cluster in bird lineages inhabiting different
654 climates. *Nat Ecol Evol* **2**, 1258–1267. (doi:10.1038/s41559-018-0606-3)

655 23. Wang S, Ore MJ, Mikkelsen EK, Lee-Yaw J, Toews DPL, Rohwer S, Irwin D. 2021 Signatures of
656 mitonuclear coevolution in a warbler species complex. *Nature Communications* **12**, 1–11.
657 (doi:10.1101/2020.04.06.028506)

658 24. Veen T, Borge T, Griffith SC, Saetre G-P, Bures S, Gustafsson L, Sheldon BC. 2001 Hybridization
659 and adaptive mate choice in flycatchers. *Nature* **411**, 45–50. (doi:10.1038/35075000)

660 25. Toews DPL, Brelsford A. 2012 The biogeography of mitochondrial and nuclear discordance in
661 animals. *Mol Ecol* **21**, 3907–3930. (doi:10.1111/j.1365-294x.2012.05664.x)

662 26. Bonnet T, Leblois R, Rousset F, Crochet P-A. 2017 A reassessment of explanations for discordant
663 introgressions of mitochondrial and nuclear genomes. *Evolution* **71**, 2140–2158.
664 (doi:10.1111/evo.13296)

665 27. Hill GE. 2019 Reconciling the Mitonuclear Compatibility Species Concept with Rampant
666 Mitochondrial Introgression. *Integr. Comp. Biol.* **59**, 912–924. (doi:10.1093/icb/icz019)

667 28. Sloan DB, Havird JC, Sharbrough J. 2017 The on-again, off-again relationship between
668 mitochondrial genomes and species boundaries. *Mol. Ecol.* **26**, 2212–2236. (doi:10.1111/mec.13959)

669 29. Stewart JB, Chinnery PF. 2015 The dynamics of mitochondrial DNA heteroplasmy: implications
670 for human health and disease. *Nat Rev Genet* **16**, 530–542. (doi:10.1038/nrg3966)

671 30. Hahn A, Zuryn S. 2019 The Cellular Mitochondrial Genome Landscape in Disease. *Trends Cell Biol*
672 **29**, 227–240. (doi:10.1016/j.tcb.2018.11.004)

673 31. Hooper DM, Griffith SC, Price TD. 2019 Sex chromosome inversions enforce reproductive
674 isolation across an avian hybrid zone. *Mol Ecol* **28**, 1246–1262. (doi:10.1111/mec.14874)

675 32. Lopez KA, McDiarmid CS, Griffith SC, Lovette IJ, Hooper DM. 2021 Evaluating evidence of
676 mitonuclear incompatibilities with the sex chromosomes in an avian hybrid zone. *Evolution* **75**,
677 1395–1414. (doi:10.1111/evo.14243)

678 33. Koch RE *et al.* 2021 Integrating Mitochondrial Aerobic Metabolism into Ecology and Evolution.
679 *Trends Ecol Evol* **36**, 321–332. (doi:10.1016/j.tree.2020.12.006)

680 34. Brazill-Boast J, van Rooij EP, Pryke SR, Griffith SC. 2011 Interference from long-tailed finches
681 constrains reproduction in the endangered Gouldian finch. *J Anim Ecol* **80**, 39–48.

682 35. Rowe M, Griffith SC, Hofgaard A, Lifjeld JT. 2015 Subspecific variation in sperm morphology and
683 performance in the Long-tailed Finch (Poephila acuticauda). *Avian Research* , 1–10.
684 (doi:10.1186/s40657-015-0032-z)

685 36. Singhal S, Leffer EM, Sannareddy K, Turner I, Venn O, Hooper DM, Strand AI. 2015 Stable
686 recombination hotspots in birds. *Science* , 1–6.

687 37. Sheldon EL, McCowan LSC, McDiarmid CS, Griffith SC. 2018 Measuring the embryonic heart rate
688 of wild birds: An opportunity to take the pulse on early development. *The Auk* **135**, 71–82.
689 (doi:10.1642/auk-17-111.1)

690 38. Martindale JL, Holbrook NJ. 2002 Cellular response to oxidative stress: Signaling for suicide and
691 survival*. *J. Cell. Physiol.* **192**, 1–15. (doi:10.1002/jcp.10119)

692 39. Birben E, Sahiner UM, Sackesen C, Erzurum S, Kalayci O. 2012 Oxidative Stress and Antioxidant
693 Defense. *World Allergy Organization J* **5**, 9–19. (doi:10.1097/wox.0b013e3182439613)

694 40. Marasco V, Stier A, Boner W, Griffiths K, Heidinger B, Monaghan P. 2017 Environmental
695 conditions can modulate the links among oxidative stress, age, and longevity. *Mech Ageing Dev* **164**,
696 100–107. (doi:10.1016/j.mad.2017.04.012)

697 41. Stier A, Romestaing C, Schull Q, Lefol E, Robin J, Roussel D, Bize P. 2017 How to measure
698 mitochondrial function in birds using red blood cells: a case study in the king penguin and
699 perspectives in ecology and evolution. *Methods Ecol Evol* **8**, 1172–1182. (doi:10.1111/2041-
700 210x.12724)

701 42. Ton R, Stier A, Cooper CE, Griffith SC. 2021 Effects of Heat Waves During Post-natal Development
702 on Mitochondrial and Whole Body Physiology: An Experimental Study in Zebra Finches. *Front Physiol*
703 **12**, 661670. (doi:10.3389/fphys.2021.661670)

704 43. Lee JC-I *et al.* 2010 A novel strategy for avian species and gender identification using the CHD
705 gene. *Mol Cell Probe* **24**, 27–31. (doi:10.1016/j.mcp.2009.08.003)

706 44. Sorenson MD, Quinn TW. 1998 Numts: A Challenge for Avian Systematics and Population
707 Biology. *Auk* **115**, 214–221. (doi:10.2307/4089130)

708 45. Valavanidis A, Vlachogianni T, FIOTAKIS C. 2009 8-hydroxy-2' -deoxyguanosine (8-OHdG): A
709 Critical Biomarker of Oxidative Stress and Carcinogenesis. *J Environ Sci Heal Part C* **27**, 120–139.
710 (doi:10.1080/10590500902885684)

711 46. Stier A, Schull Q, Bize P, Lefol E, Haussmann M, Roussel D, Robin J-P, Viblanc VA. 2019 Oxidative
712 stress and mitochondrial responses to stress exposure suggest that king penguins are naturally
713 equipped to resist stress. *Sci Rep-uk* **9**, 8545. (doi:10.1038/s41598-019-44990-x)

714 47. Stier A, Monaghan P, Metcalfe NB. 2022 Experimental demonstration of prenatal programming
715 of mitochondrial aerobic metabolism lasting until adulthood. *Proc Royal Soc B* **289**, 20212679.
716 (doi:10.1098/rspb.2021.2679)

717 48. Meiklejohn CD, Holmbeck MA, Siddiq MA, Abt DN, Rand DM, Montooth KL. 2013 An
718 Incompatibility between a Mitochondrial tRNA and Its Nuclear-Encoded tRNA Synthetase
719 Compromises Development and Fitness in Drosophila. *Plos Genet* **9**, e1003238.
720 (doi:10.1371/journal.pgen.1003238)

721 49. Li H. 2011 A statistical framework for SNP calling, mutation discovery, association mapping and
722 population genetical parameter estimation from sequencing data. *Bioinformatics* **27**, 2987–2993.
723 (doi:10.1093/bioinformatics/btr509)

724 50. Donath A, Jühling F, Al-Arab M, Bernhart SH, Reinhardt F, Stadler PF, Middendorf M, Bernt M.
725 2019 Improved annotation of protein-coding genes boundaries in metazoan mitochondrial genomes.
726 *Nucleic Acids Res* **47**, 10543–10552. (doi:10.1093/nar/gkz833)

727 51. Katoh K, Rozewicki J, Yamada KD. 2017 MAFFT online service: multiple sequence alignment,
728 interactive sequence choice and visualization. *Brief. Bioinform.* **20**, bbx108-.
729 (doi:10.1093/bib/bbx108)

730 52. Gao F, Chen C, Arab DA, Du Z, He Y, Ho SYW. 2019 EasyCodeML: A visual tool for analysis of
731 selection using CodeML. *Ecol. Evol.* **9**, 3891–3898. (doi:10.1002/ece3.5015)

732 53. Bates D, Mächler M, Bolker B, Walker S. 2015 Fitting Linear Mixed-Effects Models Using lme4. *J.*
733 *Stat. Soft.* **67**, 1-47\8. (doi:10.18637/jss.v067.i01)

734 54. Kuznetsova A, Brockhoff P, Christensen R. 2017 lmerTest Package: Tests in Linear Mixed Effects
735 Models. *Journal of Statistical Software* **82**, 1–26. (doi:10.18637/jss.v082.i13)

736 55. Lenth R. 2020 emmeans: Estimated Maringal Means, aka Least-Squares Means. R package.

737 56. Hartig F. 2021 Residual Diagnostics for Hierarchical (Multi-Level / Mixed) Regression Models [R
738 package DHARMa version 0.4.4].

739 57. Callahan B, Neher RA, Bachtrog D, Andolfatto P, Shraiman BI. 2011 Correlated Evolution of
740 Nearby Residues in Drosophilid Proteins. *Plos Genet* **7**, e1001315.
741 (doi:10.1371/journal.pgen.1001315)

742 58. Storz JF. 2018 Compensatory mutations and epistasis for protein function. *Curr Opin Struc Biol*
743 **50**, 18–25. (doi:10.1016/j.sbi.2017.10.009)

744 59. Lajbner Z, Pnini R, Camus MF, Miller J, Dowling DK. 2018 Experimental evidence that thermal
745 selection shapes mitochondrial genome evolution. *Sci Rep-uk* **8**, 9500. (doi:10.1038/s41598-018-
746 27805-3)

747 60. Lamb AM, Gan HM, Greening C, Joseph L, Lee YP, Morán-Ordóñez A, Sunnucks P, Pavlova A. 2018
748 Climate-driven mitochondrial selection: A test in Australian songbirds. *Mol Ecol* **27**, 898–918.
749 (doi:10.1111/mec.14488)

750 61. Lasne C, Heerwaarden B, Sgrò CM, Connallon T. 2019 Quantifying the relative contributions of
751 the X chromosome, autosomes, and mitochondrial genome to local adaptation*. *Evolution* **73**, 262–
752 277. (doi:10.1111/evo.13647)

753 62. Barreto FS, Burton RS. 2013 Elevated oxidative damage is correlated with reduced fitness in
754 interpopulation hybrids of a marine copepod. *Proc. R. Soc. B* **280**, 20131521–20131521.
755 (doi:10.1098/rspb.2013.1521)

756 63. Barreto FS, Watson ET, Lima TG, Willett CS, Edmands S, Li W, Burton RS. 2018 Genomic
757 signatures of mitonuclear coevolution across populations of Tigriopus californicus. *Nat Ecol Evol* **2**,
758 1250–1257. (doi:10.1038/s41559-018-0588-1)

759 64. Junker A *et al.* 2022 Human studies of mitochondrial biology demonstrate an overall lack of
760 binary sex differences: A multivariate meta-analysis. *Faseb J* **36**, e22146.
761 (doi:10.1096/fj.202101628r)

762 65. Dowling DK, Adrian RE. 2019 Challenges and Prospects for Testing the Mother's Curse
763 Hypothesis. *Integr Comp Biol* **59**, 875–889. (doi:10.1093/icb/icz110)

764 66. Carnegie L, Reuter M, Fowler K, Lane N, Camus MF. 2021 Mother's curse is pervasive across a
765 large mitonuclear Drosophila panel. *Evol Lett* **5**, 230–239. (doi:10.1002/evl3.221)

766 67. Nagarajan-Radha V, Aitkenhead I, Clancy DJ, Chown SL, Dowling DK. 2020 Sex-specific effects of
767 mitochondrial haplotype on metabolic rate in Drosophila melanogaster support predictions of the
768 Mother's Curse hypothesis. *Philosophical Transactions Royal Soc B* **375**, 20190178.
769 (doi:10.1098/rstb.2019.0178)

770 68. Cooper CE, Hurley LL, Griffith SC. 2020 Effect of acute exposure to high ambient temperature on
771 the thermal, metabolic and hygric physiology of a small desert bird. *Comp Biochem Physiology Part*
772 *Mol Integr Physiology* **244**, 110684. (doi:10.1016/j.cbpa.2020.110684)

773 69. Stier A, Metcalfe NB, Monaghan P. 2020 Pace and stability of embryonic development affect
774 telomere dynamics: an experimental study in a precocial bird model. *Proc Royal Soc B* **287**,
775 20201378. (doi:10.1098/rspb.2020.1378)

776 70. Nikelski E, Rubtsov AS, Irwin D. 2022 High heterogeneity in genomic differentiation between
777 phenotypically divergent songbirds: a test of mitonuclear co-introgression. *Heredity* , 1–13.
778 (doi:10.1038/s41437-022-00580-8)

779 71. Baris TZ, Wagner DN, Dayan DI, Du X, Blier PU, Pichaud N, Oleksiak MF, Crawford DL. 2017
780 Evolved genetic and phenotypic differences due to mitochondrial-nuclear interactions. *Plos Genet*
781 **13**, e1006517. (doi:10.1371/journal.pgen.1006517)

782 72. Nguyen THM *et al.* 2022 Mapping mitonuclear epistasis using a novel recombinant yeast
783 population. *Biorxiv* , 2022.08.31.505974. (doi:10.1101/2022.08.31.505974)

784 73. Healy TM, Burton RS. 2022 Differential gene expression and mitonuclear incompatibilities in fast-
785 and slow-developing inter-population Tigriopus californicus hybrids. *Biorxiv* , 2022.09.09.507197.
786 (doi:10.1101/2022.09.09.507197)

787 74. Healy TM, Burton RS. 2022 Genetic incompatibilities in reciprocal hybrids between populations
788 of Tigriopus californicus with low to moderate mitochondrial sequence divergence. *Biorxiv* ,
789 2022.09.19.508600. (doi:10.1101/2022.09.19.508600)

790 75. Harris DA, Das AM. 1991 Control of mitochondrial ATP synthesis in the heart. *Biochem J* **280**,
791 561–573. (doi:10.1042/bj2800561)

792 76. Wolff JN, Ladoukakis ED, Enriquez JA, Dowling DK. 2014 Mitonuclear interactions: evolutionary
793 consequences over multiple biological scales. *Philosophical Transactions of the Royal Society B:*
794 *Biological Sciences* **369**, 20130443–20130443. (doi:10.1098/rstb.2013.0443)

795 77. Hill GE. 2016 Mitonuclear coevolution as the genesis of speciation and the mitochondrial DNA
796 barcode gap. *Ecol Evol* **6**, 5831–5842. (doi:10.1002/ece3.2338)

797 78. Hill GE, Havird JC, Sloan DB, Burton RS, Greening C, Dowling DK. 2019 Assessing the fitness
798 consequences of mitonuclear interactions in natural populations. *Biol Rev* **94**, 1089–1104.
799 (doi:10.1111/brv.12493)

800 79. Pereira RJ, Lima TG, Pierce-Ward NT, Chao L, Burton RS. 2021 Recovery from hybrid breakdown
801 reveals a complex genetic architecture of mitonuclear incompatibilities. *Mol Ecol* **30**, 6403–6416.
802 (doi:10.1111/mec.15985)

803
804

Supplementary Figures

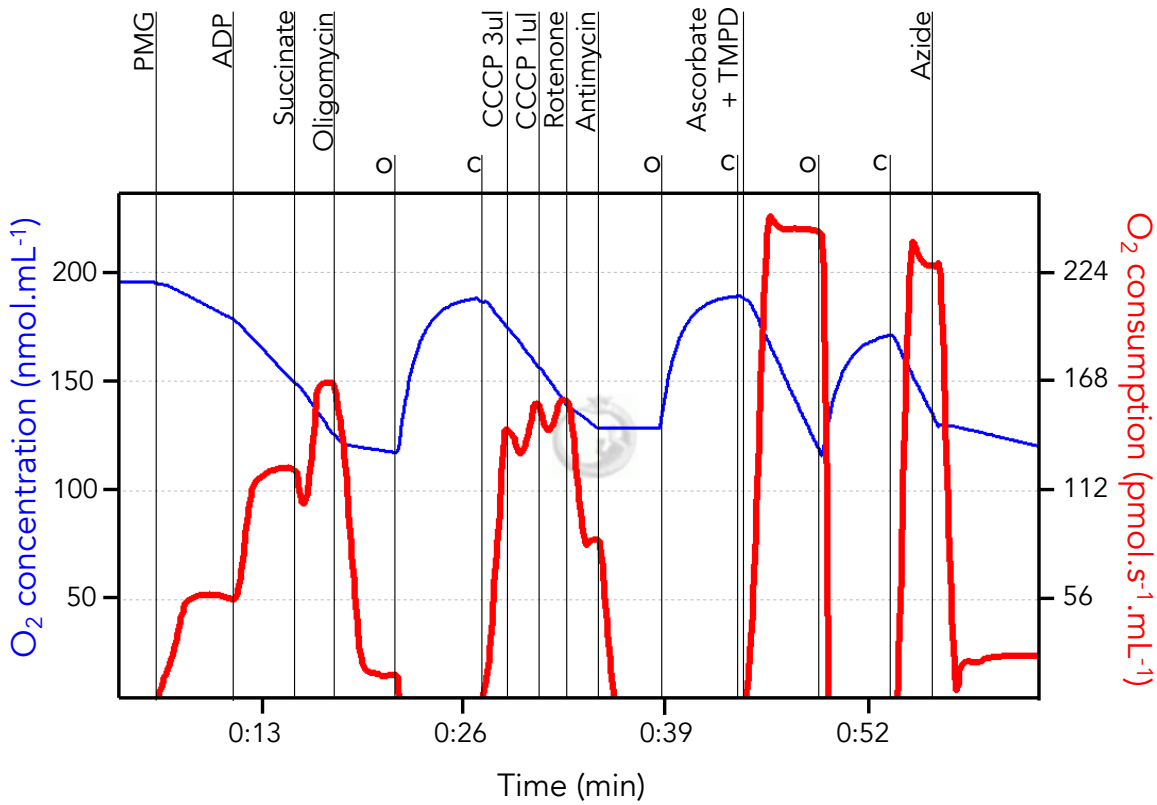

Figure S1 | Example of reading from measurement of mitochondrial respiration capacity. Oxygen concentration (blue line) and oxygen consumption (red line) following the injection of substrate, uncoupler, inhibitor titrations (SUIT) injections (long vertical lines). Chambers are opened (O) and closed (C) periodically to ensure oxygen levels do not fall too low (short lines).

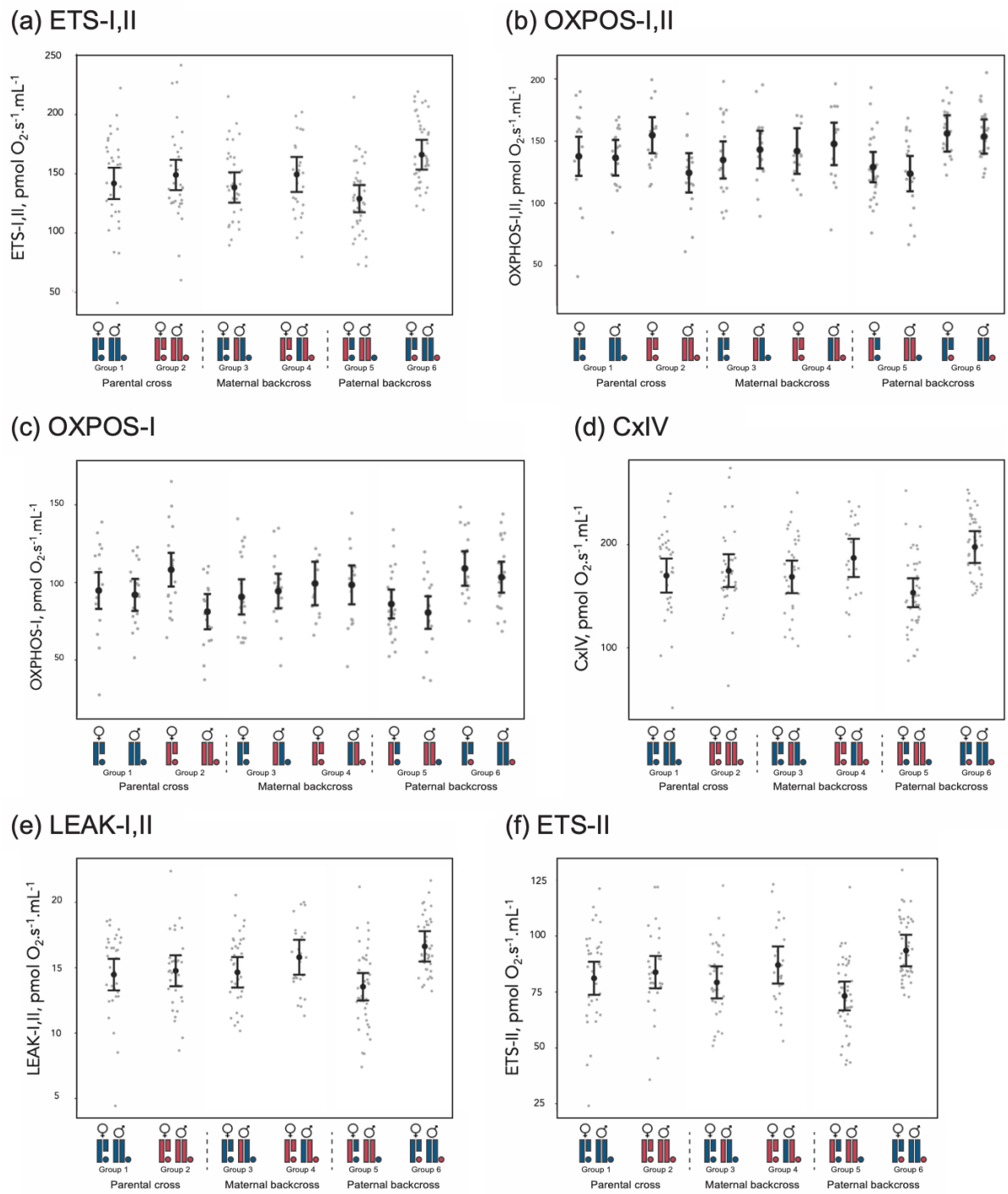

Figure S2 | High resolution respiratory data from the six measures across the six experimental groups and split by sex when there was a significant interaction (Table 3). Datapoints indicate raw data per individual, error bars are 95% CIs based on model output.

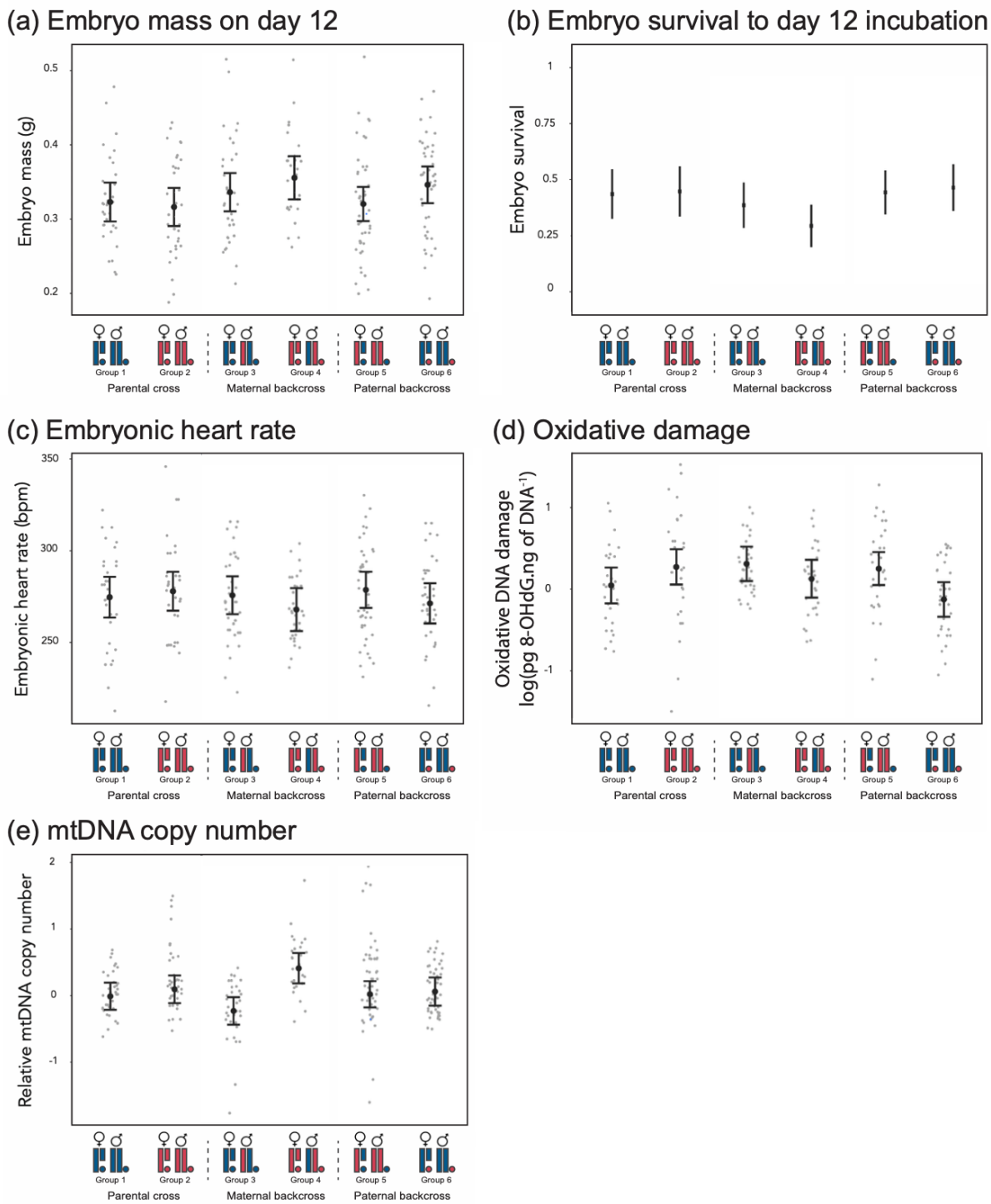

Figure S3 | Non-respiratory measures made from embryo compared across the experimental groups, where each point is the raw data from an embryo and the error bars indicate the mean and 95% CI. A: embryo mass on day 12 of incubation, B: embryo survival to day 12 incubation (yes 1, or no 0), C: embryonic heart rate, calculated from a curve generated for each embryo, here shown the predicted heart rate 60 seconds after removal from the incubator, D: 8-OHdG oxidative DNA damage, E: mtDNA copy number relative to the nuDNA copy number.